

# Exploring Hardness and Geometry Information through Active Perception

Songlin Xu<sup>1</sup>, Nan Lin<sup>2</sup>, Rui Fan<sup>2</sup>, Peichen Wu<sup>2</sup> and Xiaoping Chen<sup>2</sup>

**Abstract**—Accurate 3D reconstruction of objects has recently made great breakthroughs, thanks to the development of computer vision. Whereas precise 3D information can merely reflect an object’s geometry information, which is limited in many applications. Exploration of more information is needed to fulfill diverse tasks. As an important property of an object, hardness can provide more comprehensive information which can be widely used in various tasks like grasping and manipulation. In this paper, a framework combining active perception and motion planning algorithm is proposed to get both hardness and geometry information of an object which also ensures working efficiency. In this framework, a stylus mounted on a robotic arm explores hardness and geometry information on the surface of the object actively and a depth camera is used to capture raw 3D shape information. A novel motion planning algorithm is proposed to keep the exploration operative and time-saving. Experimental results show that our framework has good performance and can explore global hardness and geometry information efficiently.

## I. INTRODUCTION

Exploring properties of an object is a vital problem which can lead to diverse applications and tasks. As a very important property of objects, shape has attracted the attention of many researchers. Rapid advances in computer vision have made it possible for 3D precise reconstruction of objects, whether based on point cloud data [1] or images using convolutional neural network [2]. Whereas limitations still exist in 3D shape reconstruction problem with only a visual system. Thus, tactile sensors are employed to reconstruct shape in [3]. Active touch is introduced to enhance visual perception of an object’s shape [4] [5]. In fact, it can be used not only in 3D shape problem [6] [7], but also in object exploration [8] and classification [9], material perception [10], hardness recognition [11], surface recognition [12] [13] and even super resolution [14]. It can also be very helpful in some tasks like grasping [15] and manipulation [16].

The most direct information that active touch captured is actual hardness of the contact point, which can be extremely necessary in some tasks like grasping. Varley *et al.* [17] provided an architecture to enable robotic grasp planning via shape completion and Hang *et al.* [18] proposed a Fingertip Space for precision grasping. Whereas

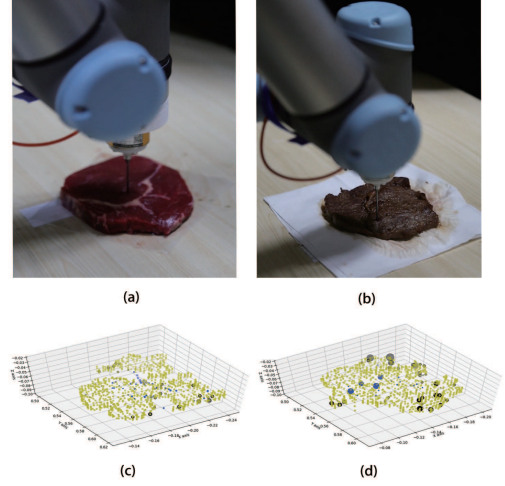


Fig. 1. (a) and (b) show that the stylus is exploring the raw steak and cooked steak respectively. (c) and (d) show the point cloud of them correspondingly. Yellow points represent original point cloud. Blue points stand for explored points and black points stand for those points whose hardness is predicted according to our algorithm. For blue and black points, the size of point reveals value of hardness. Through active touch, the hardness of the points can be explored and predicted so that we can estimate hardness of different parts of the steak. We can use the hardness information to learn whether the steak is well-cooked or not.

they both did not consider situations for objects of various changeable hardness or not consider hardness information for grasping. Kumra *et al.* [19] firstly used a deep CNN to extract features from the scene and then used a shallow CNN to predict the proper grasp configuration which improved the state-of-the art performance. However, it also only considered images as input without hardness. Thus, it’s uncertain whether it can still achieve similar performances when grasping objects of various hardness. Therefore, it is necessary to consider hardness information when robots are performing tasks.

Gemici *et al.* [20] used haptic sensors to learn physical properties including hardness to manipulate deformable food objects. But how to get precise and complete hardness of objects is still a problem. Pezzementi *et al.* [21] treated haptic exploration as a search problem in a continuous space utilizing sampling-based motion planning algorithms and used tactile data to recognize real objects. A tactile sensor can also be used to detect hardness [22] [23] [24]. Touch attention Bayesian models were developed by Martins *et al.* [25] for active haptic exploration. Caccamo *et al.* [26] used Gaussian Random Field and Gaussian Process Implicit Surfaces to explore

\*This work was supported by the National Natural Science Foundation of China under grant U1613216 and 61573333.

<sup>1</sup>Songlin Xu is with the School of Information Science and Technology, University of Science and Technology of China, Hefei, 230026, China. xsl314@mail.ustc.edu.cn

<sup>2</sup>Nan Lin, Rui Fan, Peichen Wu and Xiaoping Chen are with the School of Computer Science and Technology, University of Science and Technology of China, Hefei, 230026, China.

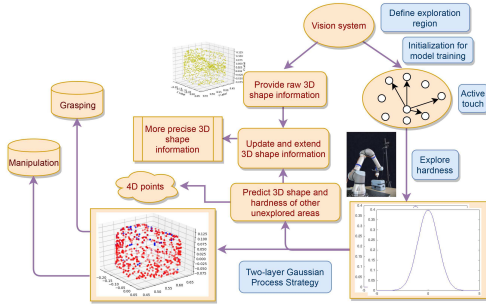


Fig. 2. Active Perception Framework

surfaces of objects. Usually force information can be used into haptic exploration [27] but this method may encounter imprecise situations and it is hard to obtain global hardness information of the object.

In this case, a framework combining active touch and vision system is proposed in this work to explore hardness of different parts of an object. Based on the raw 3D shape information collected from vision system, active touch will be employed by a stylus with a force sensor to detect global hardness information of the object as well as optimize the geometry information of the object.

Another problem is that how to plan motions of the stylus to get the hardness and geometry information within limited exploration points to save time while keeping the quality of exploration. We propose a novel sample-based motion planning algorithm based on a two-layer Gaussian Process to plan motion of the stylus to explore hardness and geometry information of an object. The algorithm can not only plan the next best sample point for hardness exploration according to former exploration results in real-time, but also predict hardness of other unexplored areas and update more precise point cloud data at the same time. In this case, the geometry information can also be updated from raw point cloud which is collected by the vision system. Finally, we validate our algorithm on several objects with various shapes and hardness. The experimental results show that the stylus can explore most parts of the object within limited exploration points. Fig. 1 demonstrates a real-life application of the exploration strategy, i.e. cooking a steak. By detecting the hardness and geometry information of the steak via active perception, we can learn whether the steak is well-cooked or not.

The contribution of this paper is as follows.

- An active perception framework combining active touch and vision system is proposed to detect hardness and geometry information of an object.
- A novel motion planning algorithm based on a two-layer Gaussian Process is developed to keep the exploration operative and efficient.
- We present the practical application with this active perception framework which is also validated in the experiment.

The rest of the paper is structured as follows. Section

II describes our methods in detail. Experiments are conducted to evaluate our algorithms in Section III. Section IV presents the conclusions and our future work.

## II. METHODOLOGIES

### A. The Active Perception Framework

The whole active perception framework is shown in Fig.2, which is mainly composed of vision and active touch system. The vision system captures raw point cloud data of the object, and active touch is performed by a stylus mounted on the tip of a robotic arm. The raw point cloud is used for initialization of our two-layer Gaussian Process algorithm as well as scaling range of movements of the stylus so that it does not have to explore the noneffective space. The two-layer Gaussian Process algorithm is developed to plan movements of the stylus to sample proper points. And the geometry information will be updated while the stylus is exploring hardness information of the object. Finally we can get 4D point data including coordinates and hardness value which can be used into further grasping and manipulation task.

### B. Sample-based Motion Planning Algorithm: A Two-layer Gaussian Process Strategy

An important problem is how to describe global hardness information of an object with explored points as few as possible. How many points are enough and what is the distribution of the points on the object? It can be too subjective if we just define them manually. We consider the hardness detection problem as a regression problem and use Gaussian Process to model hardness distribution of the object. Gaussian Process is a stochastic process, in which any finite set of random variables has a multivariate normal distribution[28]. The probability density of the normal distribution can be denoted as follows.

$$f(x|\mu, \sigma^2) = \frac{1}{\sqrt{2\pi} \times \sigma} e^{-\frac{1}{2}(\frac{x-\mu}{\sigma})^2} \quad (1)$$

where  $\mu$  is the mean of the distribution and  $\sigma$  is the standard deviation.

Our algorithm can plan the next best sample point according to previous results in real-time and also predict hardness of other unexplored areas.

1) *Basic Gaussian Process*: Each layer's Gaussian Process is based on a basic Gaussian Process, which can be trained to fit a regression problem. For a fitting problem like  $y = f(x)$ , the Gaussian Process is usually determined by the mean function  $\mu(x)$  and the kernel (covariance functions)  $k(x_i, x_j)$  which is related to the shape of Gaussian Process. Here we choose Radial-basis function (RBF) kernel as the covariance function which is denoted as follows.

$$k(x_i, x_j) = \exp(-\frac{\|x_i - x_j\|_2^2}{2l^2}) \quad (2)$$

where  $l$  is a length-scale parameter and  $l > 0$ .

We implement the basic Gaussian Process with scikit-learn [29].

2) *Two-layer Gaussian Process Strategy*: The algorithm is shown in Algorithm 1. We first define the two Gaussian Process models.

- First Layer:  $GP_1$  : In this model, the input is  $(x_i, y_i)$  and the output is  $z_i$  and  $k_i$ .  $(x_i, y_i, z_i)$  is the spatial coordinate of point  $p_i$  and  $k_i$  is hardness of this point. The fitting problem is considered as a regression problem as  $z_i = f(x_i, y_i)$  and hardness  $k_i$  is recorded at the same time. There are two purposes in  $GP_1$ :
  - Extend new point data to raw point data set of vision system to store more precise 3D shape information.
  - Get points with hardness value to initialize the second layer  $GP_2$ .
- Second Layer:  $GP_2$  : It is used to train a model to predict hardness information of the object. The regression problem is denoted as  $k_i = h(x_i, y_i, z_i)$ . The  $GP_2$  model is used with two purposes:
  - Plan sample points of active touch and get enough points with hardness to predict hardness of other unexplored areas.
  - Update point cloud data from vision system. The point cloud data can be imprecise from vision system. During the process of  $GP_2$ , positions in the point cloud can be updated to get more precise 3D shape information.

We first denote raw point cloud data set  $T_0 = [(S_1, z_1), (S_2, z_2), \dots, (S_n, z_n)]$ , where  $S_i = (x_i, y_i)$ , after we sample and segment  $n$  points from vision system. The point cloud is roughly reconstructed with appreciable error at its side face. As mentioned before, the Gaussian Process model needs initial points to start training. Unlike random selection, we introduce point cloud data  $T_0$  from vision system to initialize the first layer  $GP_1$ , thus we can get initial training data set  $T_1 = T_0$ . We set an empty set  $T_2 = \emptyset$  as initialization of the second layer  $GP_2$ . The hardness of each point explored in  $GP_1$  will be added to set  $T_2$ .

In the exploration space  $E_1 = [P_1, P_2, \dots, P_m]$  where  $P_i = (x_i, y_i)$ , we set  $Num_1$  iterations for exploration of  $GP_1$ , which means  $Num_1$  points will be explored to fit the  $GP_1$  model (The method to obtain exploration space of  $GP_1$  will be discussed later). After each training, the acquisition function will be calculated to choose the next best point  $P^* = (x^*, y^*)$ . We choose the standard deviation function  $\sigma(P)$  as the acquisition function since standard deviation presents uncertainty of the model. Then the stylus will explore the position of  $P^* = (x^*, y^*)$ . We firstly consider detecting upper surface of the object, so the motion direction of the stylus is negative direction of  $Z$  axis. Active touch is employed to detect this point and get exact  $Z$  axis coordinate of this point and more importantly, hardness  $k^*$  of this point. Then,  $(P^*, z^*)$  is added to set  $T_1$  for continuous training and  $(x^*, y^*, z^*, k^*)$  is added to set  $T_2$  for initialization of the second layer  $GP_2$ . Thus, the purpose of the first layer is to model a more precise 3D surface of the object based on the initialization of vision system and get hardness value of the explored points to

---

**Algorithm 1** The Two-layer Gaussian Process Algorithm for Active Touch Sample-based Motion Planning

---

**Input:** raw point cloud data  $T_0$

**Output:** 4D point set  $T_2$

---

**Definition**

$GP_1$  : The first layer Gaussian Process

$GP_2$  : The second layer Gaussian Process

$GP_1 : z = f(x, y)$

**Initialization:**

$T_1 = T_0 \triangleq [(S_1, z_1), (S_2, z_2), \dots, (S_n, z_n)]$ , where  $S_i = (x_i, y_i)$

$T_2 = \emptyset$

**Exploration Space:**

$E_1 = [P_1, P_2, P_3, \dots, P_m]$ , where  $P_i = (x_{new_i}, y_{new_i})$

**for** each  $i \in [1, Num_1]$  **do**

Train a 3D shape model

Calculate acquisition function  $\sigma(P)$

Find the optimal value  $P^*$  as the next sample point

Active touch on this point, get  $(P^*, z^*, k^*)$

$T_1 \leftarrow T_1 \cup (P^*, z^*)$

$T_2 \leftarrow T_2 \cup (P^*, z^*, k^*)$

**end for**

$GP_2 : k = h(x, y, z)$

**Initialization:**

$T_2 = [(P_1, z_1, k_1), (P_2, z_2, k_2), \dots, (P_{Num_1}, z_{Num_1}, k_{Num_1})]$   
where  $P_i = (x_i, y_i)$

**Exploration Space:**

$E_2 = T_0 = [(S_1, z_1), (S_2, z_2), \dots, (S_n, z_n)]$

where  $S_i = (x_i, y_i)$

**for** each  $i \in [1, Num_2]$  **do**

Train a 4D hardness model

Calculate acquisition function  $\sigma(S)$

Find the optimal value  $S^*$  as next sample point

Active touch on this point, get  $(P^*, \tilde{z}^*, k^*)$

$z \leftarrow \tilde{z}^*$

Train the 3D shape model  $GP_1$  again

$T_2 \leftarrow T_2 \cup (S^*, \tilde{z}^*, k^*)$

**end for**

**return**  $T_2$

---

initialize the second layer  $GP_2$ .

The second layer is used to model a global hardness of the object but can also update point cloud data at the same time. After  $Num_1$  iterations of  $GP_1$ , we can get the initial training data set  $T_2 = [(P_1, z_1, k_1), (P_2, z_2, k_2), \dots, (P_{Num_1}, z_{Num_1}, k_{Num_1})]$  where  $P_i = (x_i, y_i)$ . The exploration space is raw point cloud data set  $E_2 = T_0 = [(S_1, z_1), (S_2, z_2), \dots, (S_n, z_n)]$  where  $S_i = (x_i, y_i)$ . The reason why we choose raw point cloud data from depth camera vision system is that we can measure exact value of the points so that we can not only detect hardness information, but also update raw point cloud data. In this way, in each iteration of  $GP_2$ , we can update the raw point cloud data and fit model  $GP_1$  again to get a more precise

3D surface model. Besides, raw point cloud data defines a proper range in the space so that most points we choose are available and operative to perform active touch task.

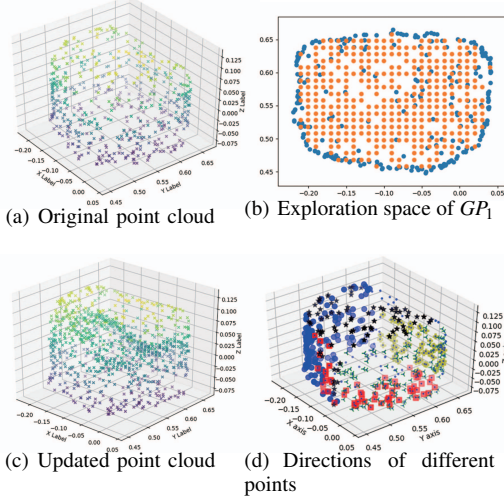


Fig. 3. (a) is the original point cloud of the object; (b) is the exploration space of  $GP_1$  generated from the winding number algorithm; (c) is the updated point cloud as the result of exploration; (d) shows the required exploring directions of different points on the object.

Based on the initial training data set  $T_2$ , we first train an initial  $GP_2$  model to fit global hardness information of the object. For each iteration (totally  $Num_2$  times) of  $GP_2$ , the acquisition function  $\sigma(S)$  will be calculated to choose the next best point  $(S^*, z^*) = (x^*, y^*, z^*)$  from data set  $E_2$ . Then active touch is performed on this point and returns new exact  $z^*$  and hardness value  $k^*$  of this point. Since the exact  $z^*$  is obtained, the updated point coordinate is added to the point cloud data set and the  $GP_1$  model is trained again based on the updated points to get more precise 3D shape model. Lastly,  $(S^*, \tilde{z}^*, k^*) = (x^*, y^*, \tilde{z}^*, k^*)$  is added to set  $T_2$  for the next iteration of  $GP_2$  model training and exploration.

3) *Decide the Exploration Space of the First Layer  $GP_1$* : Although we have raw point cloud data from vision system to initialize training of  $GP_1$  model, it is hard to decide the exploration space. If we just extract a 3D bounding box from initial point cloud data, the exploration space can be much larger than actual boundaries of the object. Some exploration points can be noneffective, which also waste time. Thus, an algorithm is needed to estimate if a 3D point is included by a point set. Since we first consider upper surface exploration with negative Z axis direction, the problem can be turned into estimating if a 2D point is included by a 2D point set which is from Z axis map of initial point cloud data set. In this case, we utilize a winding number algorithm [30] to judge if a 2D point is included by a point set and thus we can estimate if a point is valid to be explored. Fig.3 (a) shows original point cloud of the object and Fig.3 (b) shows the result of the winding number algorithm. The blue points are boundaries of initial point cloud and orange points stand for the exploration space generated by the winding

number algorithm.

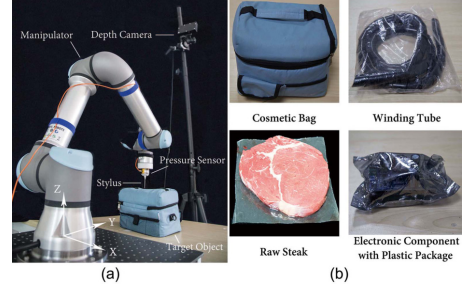


Fig. 4. (a) shows the experimental setup. (b) shows the four objects (cosmetic bag, winding tube, raw steak and electronic component with plastic package) chosen for hardness exploration.

### C. Multi-surface Hardness Detection with the Two-layer Gaussian Process Strategy

The previous section discussed exploration on the upper surface with the direction of negative Z axis. It is more complex but necessary to think about multi-surface where we should set various directions for each facet of the object. Hence, we design five directions  $(x+, x-, y+, y-, z-)$  to explore upper surface and lateral surfaces. But it is hard to choose proper direction for the robotic arm to move to the point that will be explored. Thus, a distance-based method is proposed to plan motion directions of the robotic arm according to the position of point to be explored.

#### 1) Method to Determine Direction of Exploration:

We designed five directions of the object to detect:  $(x+, x-, y+, y-, z-)$ . For each point  $p^*$ , we consider the best robot-arm-pose for the stylus to explore the point directly. A tiny bounding box around  $p^*$  is used to estimate if there is any point blocking the stylus. If not, the direction can be used for exploration. Otherwise it needs to check if  $p^*$  is closed enough to this facet. If not, it had to check other directions. The result of this method is shown in Fig.3 (d). Different marks represent different exploring directions.

#### 2) Multi-surface Situation for Active Touch:

The multi-surface situation is based on single-surface situation. The stylus will firstly explore upper surface and use the obtained hardness and point data to continue exploration of lateral surfaces. The lateral surface exploration will continue using  $GP_2$ . The input is  $(x_i, y_i, z_i)$  and the output is  $k_i$ . The exploration direction is mentioned in the previous section, which is different from single surface exploration. Then the stylus can detect hardness of multi-surface situations and finally get global hardness information. Besides, the geometry information is updated at the same time.

## III. EXPERIMENTS AND ANALYSIS

### A. Experimental Setup

Experimental setup is shown in Fig. 4(a). A depth camera (percipio.xyz, FM830-5M, 2mm measuring accuracy), whose view can cover the whole experiment table, is fixed



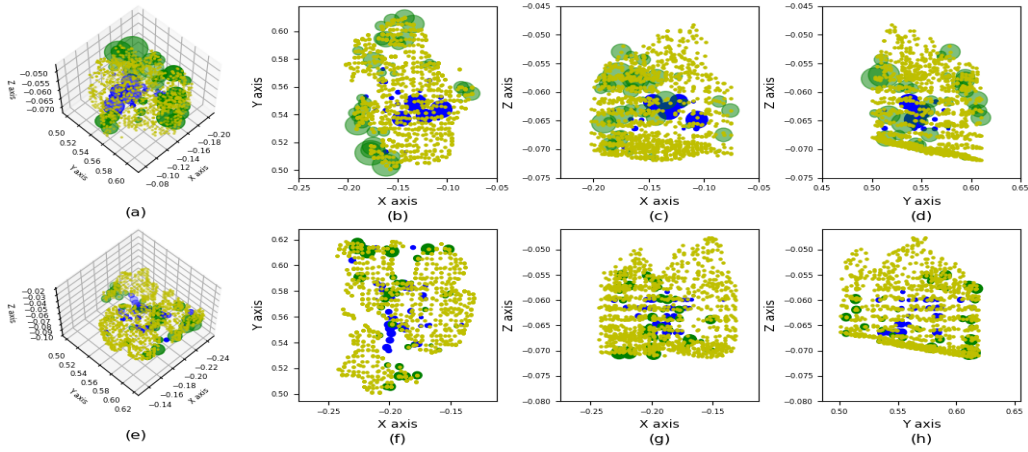


Fig. 5. (a) and (e) represent 3D point cloud with hardness information of cooked steak and raw steak respectively. Yellow points stand for original point cloud. Blue and green points stand for the explored points and predicted points respectively. For blue and green points, the size of point reveals the value of hardness. (b)(c)(d) show the different views from X-Y axis, X-Z axis and Y-Z axis of (a) respectively. (f)(g)(h) show the different views from X-Y axis, X-Z axis and Y-Z axis of (e) respectively.

to a tripod opposite the six-axis robotic arm (Universal Robots, UR5e, 0.03mm pose repeatability). A high-precision pressure sensor (freud, DHMH-106, 1% F.S., 1kg Max) is mounted on the tip of the manipulator. The other side of the sensor is connected to a stylus (Renishaw, A-5000-7521, 5mm ruby ball styli). The pressure sensor has been well calibrated and gravity-compensated. We prepare four objects for the experiments which are shown in Fig.4(b).

In the experiment, when the stylus contacts with the object, the force will be detected. The contact depth increases along with the tiny normal displacement of the manipulator, and the applied force gradually increases correspondingly. The slope of the force-displacement curve approximately represents the hardness of the target object. More specifically, before collision, the manipulator continuously approaches the contact point estimated by point cloud. When the measurement value of pressure sensor surpasses a threshold (0.02N), we consider that the stylus has touched the target object. The contact point is recorded as the real outer contour point of the object. Then the manipulator moves 4mm deeper along the normal direction, and records the pressure value every 0.4mm during the process. Eventually the slope is calculated using least square method.

#### B. Global Hardness Exploration to Distinguish between Raw Steak and Cooked Steak

We set up a task to distinguish between raw steak and cooked steak to validate our global hardness exploration algorithm. A raw steak was explored first. We used point cloud of raw steak obtained from the depth camera to initialize the two-layer Gaussian Process strategy and then started active touch exploration. During each iteration, the stylus would explore one point on the surface of the object and then decided next best exploration point from previous data of hardness and positions. After finishing exploration of raw steak, the steak was cooked and then the hardness

of different parts was explored again.

The results are shown in Fig.5. Fig.5 (a) and (e) are the 3D point cloud with hardness information of cooked and raw steak respectively. The yellow points are point clouds from depth camera. The blue points are the explored points and hardness of green points is predicted from the model we developed. The hardness value of blue points and green points are represented by the size of the point marker and larger point marker means the point with larger hardness value. Fig.5 (b)(c)(d) show the different views from X-Y axis, X-Z axis and Y-Z axis of (a) respectively and (f)(g)(h) show the different views from X-Y axis, X-Z axis and Y-Z axis of (e) respectively. From the result we can find that the explored and predicted points distribute evenly on the object. And it is obvious that cooked steak is harder than raw steak.

From Fig.5 we can get the conclusions as follows.

- Our algorithm can plan sample points of different surfaces of the object. Besides, the points do not centrally distribute on a single surface or area which can ensure that the stylus can explore global hardness information of the object but not only a local area.
- The hardness of cooked steak and raw steak can be distinguished clearly with global hardness exploration which reveals good performance of our algorithm. Besides, the result that cooked steak is harder than raw steak also meets people's common sense.
- The experiment shows that our framework has practical application value like estimating if the food is well-cooked.

#### IV. CONCLUSIONS AND FUTURE WORK

In this paper, we propose an active perception framework combining active touch and vision system to explore hardness and geometry information of objects. Additionally, a novel improved two-layer Gaussian Process based algorithm is developed to plan sample points of

exploration efficiently and the algorithm can also estimate hardness of other unexplored areas properly which can help us obtain global hardness information of the object. And geometry information from raw point cloud can be updated in real time when the hardness information is being explored so that we can get more precise geometry information of objects. Besides, the experiments show the practical applications of our active perception framework like learning if the food is well-cooked when cooking.

One of the future works is to utilize the hardness and geometry information to help robots perform grasping and manipulation task more accurately and efficiently. Besides, high-resolution RGB camera can capture tiny shape deformation when active touch is conducted on the object. And we will explore the fusion of active vision and active touch system to capture the tiny deformation to obtain more precise hardness and geometry information in the future.

## REFERENCES

- [1] R. B. Rusu and S. Cousins, "3d is here: Point cloud library (pcl)," in *2011 IEEE International Conference on Robotics and Automation*, May 2011, pp. 1–4.
- [2] A. S. Jackson, A. Bulat, V. Argyriou, G. Tzimiropoulos, A. S. Jackson, A. Bulat, V. Argyriou, G. Tzimiropoulos, A. S. Jackson, and A. Bulat, "Large pose 3d face reconstruction from a single image via direct volumetric cnn regression," pp. 1031–1039, 2017.
- [3] M. Moll and M. A. Erdmann, "Reconstructing shape from motion using tactile sensors," vol. 2, 02 2001, pp. 692 – 700 vol.2.
- [4] M. Bjorkman, Y. Bekiroglu, V. Hogman, and D. Kragic, "Enhancing visual perception of shape through tactile glances," in *Ieee/rsj International Conference on Intelligent Robots and Systems*, 2013, pp. 3180–3186.
- [5] Z. Yi, R. Calandra, F. Veiga, H. van Hoof, T. Hermans, Y. Zhang, and J. Peters, "Active tactile object exploration with gaussian processes," in *2016 IEEE/RSJ International Conference on Intelligent Robots and Systems (IROS)*, Oct 2016, pp. 4925–4930.
- [6] U. Martinez-Hernandez and T. J. Prescott, "Adaptive perception: Learning from sensory predictions to extract object shape with a biomimetic fingertip," in *2017 IEEE/RSJ International Conference on Intelligent Robots and Systems (IROS)*, Sep. 2017, pp. 6735–6740.
- [7] C. Strub, F. Wörgötter, H. Ritter, and Y. Sandamirskaya, "Using haptics to extract object shape from rotational manipulations," in *2014 IEEE/RSJ International Conference on Intelligent Robots and Systems*, Sep. 2014, pp. 2179–2186.
- [8] C. Yang and N. F. Lepora, "Object exploration using vision and active touch," in *2017 IEEE/RSJ International Conference on Intelligent Robots and Systems (IROS)*, Sep. 2017, pp. 6363–6370.
- [9] P. Güler, Y. Bekiroglu, X. Gratal, K. Pauwels, and D. Kragic, "What's in the container? classifying object contents from vision and touch," in *2014 IEEE/RSJ International Conference on Intelligent Robots and Systems*, Sep. 2014, pp. 3961–3968.
- [10] W. Yuan, Y. Mo, S. Wang, and E. H. Adelson, "Active clothing material perception using tactile sensing and deep learning," *CoRR*, vol. abs/1711.00574, 2017. [Online]. Available: <http://arxiv.org/abs/1711.00574>
- [11] M. Johnsson and C. Balkenius, "Recognizing texture and hardness by touch," in *2008 IEEE/RSJ International Conference on Intelligent Robots and Systems*, Sep. 2008, pp. 482–487.
- [12] R. Ibrayev and Y. Jia, "Recognition of curved surfaces from "one-dimensional" tactile data," *IEEE Transactions on Automation Science and Engineering*, vol. 9, no. 3, pp. 613–621, July 2012.
- [13] Y. Gao, L. A. Hendricks, K. J. Kuchenbecker, and T. Darrell, "Deep learning for tactile understanding from visual and haptic data," *CoRR*, vol. abs/1511.06065, 2015. [Online]. Available: <http://arxiv.org/abs/1511.06065>
- [14] N. F. Lepora and B. Ward-Cherrier, "Superresolution with an optical tactile sensor," in *2015 IEEE/RSJ International Conference on Intelligent Robots and Systems (IROS)*, Sep. 2015, pp. 2686–2691.
- [15] R. Krug, A. J. Lilienthal, D. Kragic, and Y. Bekiroglu, "Analytic grasp success prediction with tactile feedback," in *2016 IEEE International Conference on Robotics and Automation (ICRA)*, May 2016, pp. 165–171.
- [16] L. Cramphorn, B. Ward-Cherrier, and N. F. Lepora, "Tactile manipulation with biomimetic active touch," in *2016 IEEE International Conference on Robotics and Automation (ICRA)*, May 2016, pp. 123–129.
- [17] J. Varley, C. DeChant, A. Richardson, A. Nair, J. Ruales, and P. K. Allen, "Shape completion enabled robotic grasping," *CoRR*, vol. abs/1609.08546, 2016. [Online]. Available: <http://arxiv.org/abs/1609.08546>
- [18] K. Hang, J. A. Stork, and D. Kragic, "Hierarchical fingertip space for multi-fingered precision grasping," in *2014 IEEE/RSJ International Conference on Intelligent Robots and Systems*, Sep. 2014, pp. 1641–1648.
- [19] S. Kumra and C. Kanan, "Robotic grasp detection using deep convolutional neural networks," *CoRR*, vol. abs/1611.08036, 2016. [Online]. Available: <http://arxiv.org/abs/1611.08036>
- [20] M. C. Gemici and A. Saxena, "Learning haptic representation for manipulating deformable food objects," in *2014 IEEE/RSJ International Conference on Intelligent Robots and Systems*, Sep. 2014, pp. 638–645.
- [21] Z. Pezzementi, E. Plaku, C. Reyda, and G. D. Hager, "Tactile-object recognition from appearance information," *IEEE Transactions on Robotics*, vol. 27, no. 3, pp. 473–487, June 2011.
- [22] M. Shikida, T. Shimizu, K. Sato, and K. Itoigawa, "Active tactile sensor for detecting contact force and hardness of an object," *Sensors and Actuators A: Physical*, vol. 103, no. 1, pp. 213 – 218, 2003, micromechanics section of Sensors and Actuators, based on contributions revised from the Technical Digest of the 15th IEEE International conference on Micro Electro mechanical Systems (MEMS 2002). [Online]. Available: <http://www.sciencedirect.com/science/article/pii/S0924424702003369>
- [23] W. Yuan, M. A. Srinivasan, and E. H. Adelson, "Estimating object hardness with a gelsight touch sensor," in *2016 IEEE/RSJ International Conference on Intelligent Robots and Systems (IROS)*, Oct 2016, pp. 208–215.
- [24] W. Yuan, C. Zhu, A. Owens, M. A. Srinivasan, and E. H. Adelson, "Shape-independent hardness estimation using deep learning and a gelsight tactile sensor," *CoRR*, vol. abs/1704.03955, 2017. [Online]. Available: <http://arxiv.org/abs/1704.03955>
- [25] R. Martins, J. F. Ferreira, and J. Dias, "Touch attention bayesian models for robotic active haptic exploration of heterogeneous surfaces," *CoRR*, vol. abs/1409.6226, 2014. [Online]. Available: <http://arxiv.org/abs/1409.6226>
- [26] S. Caccamo, Y. Bekiroglu, C. H. Ek, and D. Kragic, "Active exploration using gaussian random fields and gaussian process implicit surfaces," in *2016 IEEE/RSJ International Conference on Intelligent Robots and Systems (IROS)*, Oct 2016, pp. 582–589.
- [27] R. S. Jamisola, P. Kormushev, A. Bicchì, and D. G. Caldwell, "Haptic exploration of unknown surfaces with discontinuities," in *2014 IEEE/RSJ International Conference on Intelligent Robots and Systems*, Sep. 2014, pp. 1255–1260.
- [28] D. J. MacKay and D. J. Mac Kay, *Information theory, inference and learning algorithms*. Cambridge university press, 2003.
- [29] F. Pedregosa, G. Varoquaux, A. Gramfort, V. Michel, B. Thirion, O. Grisel, M. Blondel, P. Prettenhofer, R. Weiss, V. Dubourg, J. Vanderplas, A. Passos, D. Cournapeau, M. Brucher, M. Perrot, and E. Duchesnay, "Scikit-learn: Machine learning in Python," *Journal of Machine Learning Research*, vol. 12, pp. 2825–2830, 2011.
- [30] K. Hormann and A. Agathos, "The point in polygon problem for arbitrary polygons," *Computational Geometry*, vol. 20, no. 3, pp. 131 – 144, 2001. [Online]. Available: <http://www.sciencedirect.com/science/article/pii/S0925772101000128>